Single and multi-quasiparticle states in ^{181}Ta from incomplete fusion

G. D. Dracoulis,[1] A. P. Byrne,[1,2] S. M. Mullins,[1] T. Kibédi,[1] F. G. Kondev,[1] and P. M. Davidson[1]
[1]*Department of Nuclear Physics, Research School of Physical Sciences and Engineering, Australian National University, Canberra, A.C.T. 0200, Australia*
[2]*Department of Physics and Theoretical Physics, Australian National University, Canberra, A.C.T. 0200, Australia*
(Received 6 April 1998)

Excited states in ^{181}Ta have been identified using time-correlated γ-ray spectroscopy and particle-γ techniques following the incomplete fusion reaction ^{176}Yb(^{11}B,$\alpha 2n$)^{181}Ta. As well as observing the rotational band based on the 11 ns isomer at 482 keV from the $5/2^+[402]$ proton configuration, which is found to be essentially identical to that associated with its $7/2^+[404]$ pseudospin partner, several multi-quasiparticle isomers are observed including a 33 μs state, of probable spin and parity $21/2^-$, at 1483 keV. Experimental states are compared with multi-quasiparticle calculations. [S0556-2813(98)02909-4]

PACS number(s): 21.10.Tg, 23.20.Lv, 27.70.+q, 21.10.Ky

Collective and intrinsic states of high or even medium spins in nuclei close to stability are at present of limited accessibility via fusion-evaporation reactions. Incomplete fusion reactions, in which the projectile breaks up into an α particle which continues with the beam velocity and a more massive fragment which fuses with the target nucleus, provide a means of reaching some such cases. The cross sections are larger than expected on the basis of evaporation of an α particle from the compound system and the reaction retains some of the characteristics of fusion, neutron evaporation for the component of the reaction involving the fragment.

The results here for the stable nucleus ^{181}Ta, were obtained from measurements concentrated on the study of ^{180}Ta [1,2] for which we have carried out studies with both the ^{176}Yb(^{7}Li,3n)^{180}Ta reaction which is essentially subbarrier, and where no significant yield of ^{181}Ta was observed, and the ^{176}Yb(^{11}B,$\alpha 3n$)^{180}Ta reaction where the competing $\alpha 2n$ channel leads to ^{181}Ta. Beams were provided by the 14UD Pelletron accelerator and were incident on metal targets of thickness 4.6 mg cm^{-2} enriched to 97% in ^{176}Yb. In the latter bombardment, the pure $4n$ evaporation channel leading to ^{183}Re is optimum at a beam energy of about 55 MeV. At that energy, approximately 10% of the yield goes into the channels involving α emission, mainly to ^{180}Ta ($\alpha 3n$) but partly to ^{181}Ta ($\alpha 2n$), which is much larger than the proportion expected for evaporation α particles. The optimum energy for ^{180}Ta is higher, about 65 MeV and as discussed recently [3], the product involving fewer neutrons emitted is correlated with the emission of more-forward angle α particles, allowing partial selection of ^{181}Ta.

In the main measurements charged particles were detected in a compact array of scintillators inserted inside the γ-ray array CAESAR [4] which has six Compton suppressed Ge detectors arranged in a plane. The particle-detector array [5] contains 14 fast/slow combined plastic scintillators for which the phoswich technique is used to separate the fast signals in the thin front element (ΔE) from the thicker (slow) rear element (E). The array covers approximately 85% of 4π and for the experiments, various gold or aluminum absorber foils were used on the four forward detectors to reduce the flux from scattered beam particles. There are three rings of essentially equivalent detectors, four "forward," six "middle," and four "backward" subtending angles of approximately $20°-60°$, $60°-120°$, and $120°-165°$. Time-filtered ΔE signals [6] concatinated into three groups were recorded for gating.

The event-by-event data, including all relative time information with time differences up to ± 856 ns, were arranged into matrices for gating on individual γ rays with different time conditions. Chopped beam measurements tailored for the measurement of long lifetimes were also performed [1]. The level scheme obtained is summarized in Fig. 1.

One-quasiparticle states. Rotational bands based on the $7/2^+[404]$ and $9/2^-[514]$ one-quasiparticle states are confirmed and extended in spin by a few units from those known from previous work (see Ref. [7]), predominantly Coulomb excitation. The $5/2^+[402]$ isomeric state at 482 keV was known but its rotational band had not been observed. A spectrum of γ rays in coincidence with the 482 keV transition that depopulates the bandhead is shown in Fig. 2(a). Analysis of the measured in-band γ-ray branching ratios using standard rotational model formulas give a value of g_K-g_R $=1.25\pm 0.11$, which is consistent with the expected value of g_K of 1.57 for the $5/2^+[402]$ configuration and $g_R \sim +0.3$.

It is noteworthy that the in-band $9/2^+ \rightarrow 7/2^+$, $11/2^+ \rightarrow 9/2^+$, $13/2^+ \rightarrow 11/2^+$, and $15/2^+ \rightarrow 13/2^+$ transitions are very close in energy to transitions in the $7/2^+[404]$ band. The $5/2^+[402]$ and $7/2^+[404]$ configurations are pseudospin partners whose excited states usually mix when the bands lie close together, resulting in perturbation of the transition energies. The similarity of the $5/2^+[402]$ and $7/2^+[404]$ bands in the series of lutetium isotopes ^{173,175,177}Lu where these orbitals also have energy separations of $\sim$400 keV because of the lower proton Fermi surface, has been noted in the review of identical bands presented by Baktash, Haas, and Nazarewicz [8]. The 994 keV state which feeds the $5/2^+[402]$ bandhead does not have an associated rotational band defined but it could be an intrinsic state, possibly from the $3/2^+$ [411] orbital which arises from the same spherical parent ($d_{5/2}$) and which, on the basis of calculations described below, is expected at about 1060 keV.

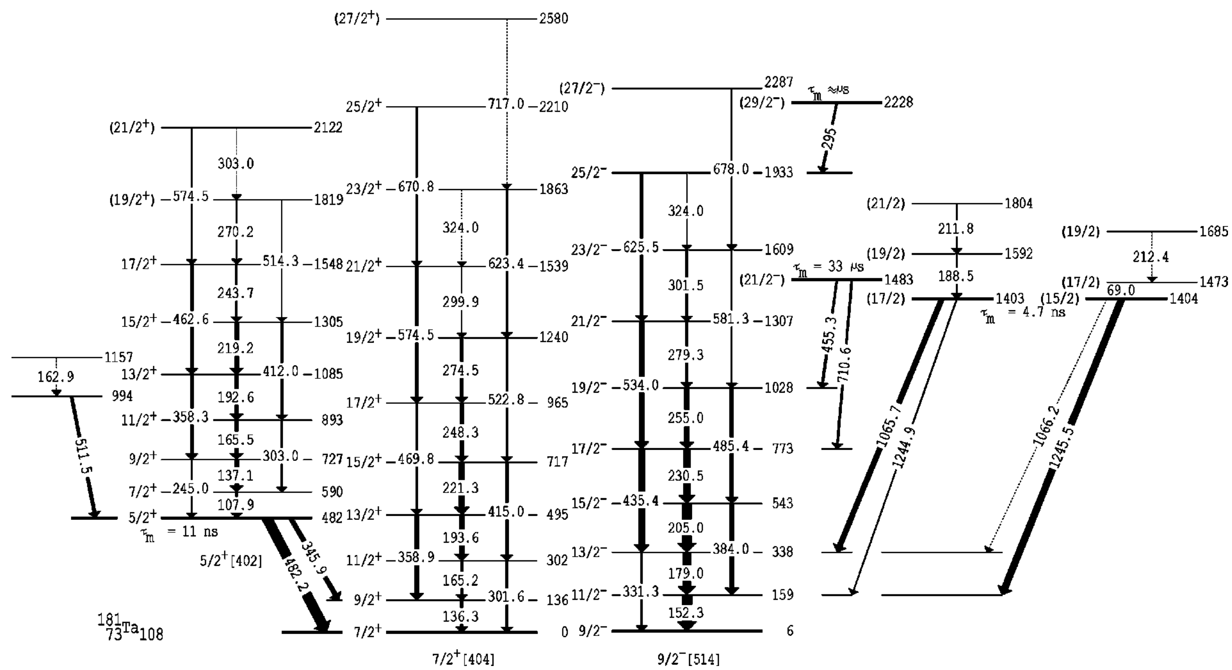

FIG. 1. Level scheme for ^{181}Ta observed in the present study. The widths of the transitions correspond approximately to the relative γ-ray intensity observed at the 55 MeV beam energy.

Three-quasiparticle intrinsic states. A long-lived state at 1483 keV feeds in to the $9/2^-[514]$ band, predominantly via the 455 keV transition to the $19/2^-$ state (a 72% γ-ray branch) and also via a 711 keV transition to the $17/2^-$ state.

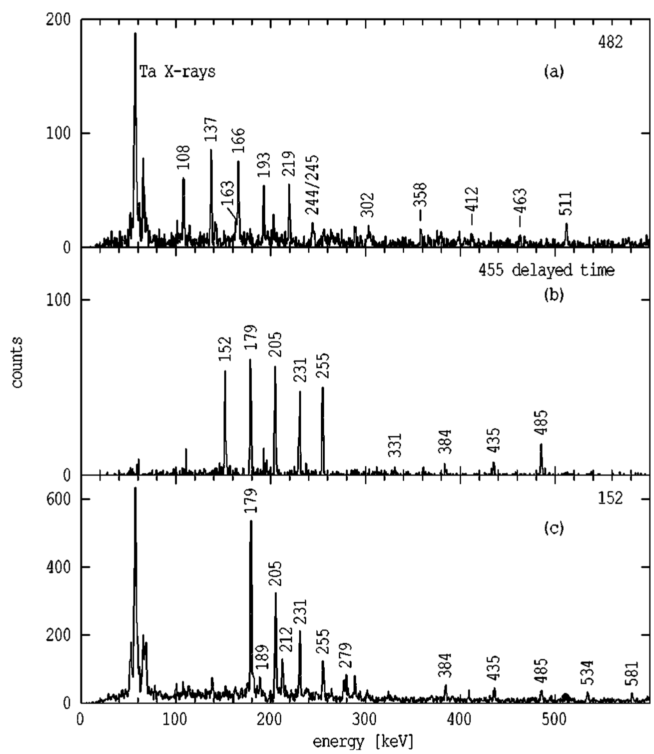

FIG. 2. Coincidence γ-ray spectra. (a) Spectrum in coincidence with α-particles and also the 482 keV transition in the time interval ± 120 ns. (b) Spectrum in prompt coincidence with the 455 keV transition, with the condition that all transitions occur between beam pulses. The relative time condition here is ± 20 ns which reduces the efficiency in the x-ray region. (c) Spectrum in prompt coincidence with α particles and the 152 keV transition.

A delayed gate on the 455 keV transition is shown in Fig. 2(b). The time curve shown in Fig. 3, obtained from chopped beam measurements [1] gives a meanlife of 33^{+8}_{-3} μs.

On the basis of the decay branches and the possible transition strengths, the likely spins and parities are $21/2^{\pm}$ or $23/2^{\pm}$, but consideration of the reduced K-hindrance factors per degree of K forbiddenness for the 455 and 711 keV transitions leads to elimination of most of these alternatives. This factor f_{ν}, defined for transitions of multipole order λ and forbiddenness $\nu = \Delta K$-λ, is given by $f_{\nu} = (T^{\gamma}/T^{W})^{1/\nu} = (f)^{1/\nu}$, with T^W being the Weisskopf single particle estimate and f the corresponding hindrance factor. Consideration of the values so obtained means that spin and parity $21/2^+$ can be eliminated on the basis of the extreme hindrance implied for the 455 keV transition (which would be $E1$, with $f_{\nu} = 107$); $23/2^+$ leads to abnormally strong $M2$ and $E3$ values for the the 455 and 711 keV transitions, and

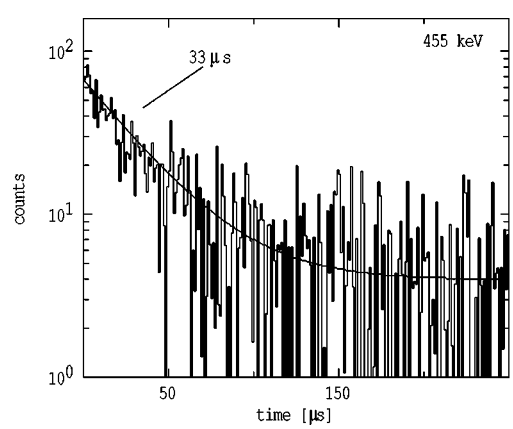

FIG. 3. Time spectrum for the 455 keV transition in the chopped beam experiment, fitted to obtain the meanlife indicated.

$23/2^-$ would imply an enhanced, 711 keV $M3$ transition. This leaves only the $21/2^-$ alternative with f_ν values of 42 and 36 for the 455 and 711 keV transitions, respectively. There is also evidence of delayed feeding to the $25/2^-$ state via a 295 keV transition, from a state tentatively assigned as $29/2^-$ (multipolarities higher than $E2$ would have prohibitively large conversion coefficients) but a definitive lifetime could not be obtained because of low population, although it is possibly in the region of many microseconds.

Several other states are observed near 1404 keV, at least one of which has a short lifetime ~ 5 ns. Two close states are shown in the scheme at 1403 and 1404 keV, both decaying by 1066 and 1245 keV transitions to the $13/2^-$ and $11/2^-$ states of the $9/2^-$ band, but with different branching ratios, implying different spins. This complication was necessitated by the γ-γ coincidence data which are not consistent with the decay of a single state. Neither were the intensities of the transitions above these states, specifically the 189 and 212 keV γ rays, consistent with a single cascade, or decay into a single state. Unfortunately because of limited population we have not been able to precisely define the level scheme in this region. The situation is further complicated by self coincidences which indicate the presence of at least two 212 keV transitions and also a 69 keV line in this part of the scheme, possibly an $E1$ transition from another intrinsic state.

The maximum spins consistent with the short lifetimes are $17/2^-$ for the state that decays mainly to the $13/2^-$ state and 15/2 for the other. The $E2$ strength in the former case would be $2.1(5)\times 10^{-3}$ W.u. corresponding to an f_ν value of 22, reasonable for such a state.

Multi-quasiparticle calculations. Selected intrinsic states predicted from multi-quasiparticle calculations are listed in Table I. These were carried out using the methods described in detail in Ref. [9] which treats the systematics of the odd tantalum isotopes from ^{175}Ta to ^{179}Ta. The calculations begin with the Nilsson levels at the calculated equilibrium deformations [10], to produce a set of basis states. For a chosen pairing interaction, the calculated levels near the Fermi surface are first adjusted to approximately reproduce the observed one-quasiparticle states (in the present case the average of the observed one-quasineutron states in ^{179}Hf and ^{181}W) and no further adjustments are made. The Lipkin-Nogami prescription is used with blocking and particle number conservation, as in the formalism described by Nazarewicz *et al.* [11]. Residual interactions in the multiparticle states are subsequently added to the predicted energies. The results are particularly sensitive to the position of the single neutron levels because, in this region the Fermi level falls between the $7/2^-[514]$ and $7/2^-[503]$ neutron states whose energies change rapidly with deformation.

A number of configurations likely to produce intrinsic states which could compete with the collective states that form the one-quasiparticle bands are predicted, but each is affected significantly by the effect of residual interactions deduced using the prescriptions of Ref. [12], which are also listed in the table. For example the predicted ordering of the two lowest $23/2^-$ states (from $\nu^2\pi$ configurations) is inverted by the addition of a large repulsive interaction to one, and an attractive interaction to the other.

TABLE I. Selected three- and five-quasiparticle states in ^{181}Ta.

K^π	Configuration [a] ν	Configuration [a] π	E_{qp}	E_{res} (keV)	E_{calc}	E_{expt}
$15/2^+$	$7/2^-$ $1/2^{-\prime}$	$7/2^+$	1660	−265	1395	(1404)
$17/2^-$	$9/2^+$ $1/2^{-\prime}$	$7/2^+$	1307	+265	1572	(1473)
$17/2^-$	$7/2^-$ $1/2^{-\prime}$	$9/2^-$	1663	−210	1453	1403
$19/2^-$	$9/2^+$ $3/2^-$	$7/2^+$	1525	−138	1387	
$19/2^+$	$9/2^+$ $1/2^{-\prime}$	$9/2^-$	1311	+8	1319	
$21/2^+$	$9/2^+$ $3/2^-$	$9/2^-$	1529	−145	1384	
$21/2^-$		$9/2^-$ $7/2^+$ $5/2^+$	1673	−77	1596	1483
$23/2^-$	$9/2^+$ $7/2^{-\prime}$	$7/2^+$	1592	+310	1902	
$23/2^-$	$7/2^-$ $7/2^{-\prime}$	$9/2^-$	1931	−166	1765	
$25/2^+$	$9/2^+$ $7/2^{-\prime}$	$9/2^-$	1595	+6	1601	
$29/2^-$	$9/2^+$ $11/2^+$	$9/2^-$	2204	−14	2185	2228
$37/2^+$	$9/2^+$ $7/2^{-\prime}$	$9/2^-$ $7/2^+$ $5/2^+$	3365	−144	3220	

[a]Configurations: (π): $9/2^-$:$9/2^-[514]$; $7/2^+$:$7/2^+[404]$; $5/2^+$:$5/2^+[402]$; $1/2^+$:$1/2^+[411]$; $1/2^-$:$1/2^-[541]$. (ν): $1/2^-$:$1/2^-[521]$; $9/2^+$:$9/2^+[624]$; $5/2^-$:$5/2^-[512]$; $7/2^-$:$7/2^-[514]$; $7/2^{-\prime}$:$7/2^-[503]$; $1/2^{-\prime}$:$1/2^-[510]$; $3/2^-$:$3/2^-[512]$.

The configuration for the $21/2^-$ state given in Table I and presumably to be identified with the observed isomer at 1483 keV is π^3, involving the three proton orbitals closest to the Fermi surface. Its rotational band would be distinctive because of the large g_K for such a configuration, leading to dominance of cascade transitions, in contrast to the bands associated with the other three-quasiparticle states (nearly all $\nu^2\pi$) predicted. The $19/2^-$, $19/2^+$ states predicted between 1300 and 1400 keV would be unlikely to result in isomers, however, a state which is yrast and could be populated is the $25/2^+$ state calculated near 1600 keV, as yet not identified.

A favored three-quasiparticle state with $K=29/2^-$ state is predicted at about 2185 keV, clear from any others and a candidate for the observed isomer at 2228 keV. The energy match may be fortuitous although equivalent calculations also correctly predict the energy of the 10^+ isomer in ^{182}W, observed at 2230 keV [13], which has the same configuration except for the additional $9/2^-[514]$ proton. Although out of reach of these kind of experiments, a five-quasiparticle state, with $K=37/2^+$, is predicted to be yrast and is likely to be long lived.

The academic and technical staff of the ANU 14UD accelerator facility are thanked for their support. Dr. G. J. Lane and Mr T. McGoram contributed to some parts of the data collection and analysis.

[1] G.D. Dracoulis, F.G. Kondev, A.P. Byrne, T. Kibédi, S. Bayer, and P.M. Davidson, Phys. Rev. C **53**, 1205 (1996).

[2] G.D. Dracoulis, S.M Mullins, A.P. Byrne, F.G. Kondev, T. Kibédi, S. Bayer, P.M. Davidson, T. McGoram, and G.J. Lane, this issue, Phys. Rev. C **58**, 1444 (1998).

[3] G.D. Dracoulis, A.P. Byrne, T. Kibédi, T.R. McGoram, and S.M. Mullins, J. Phys. G **23**, 1191 (1997).

[4] G.D. Dracoulis and A.P. Byrne, Department of Nuclear Physics Annual Report No. ANU-P/1052, 1989 (unpublished).

[5] G.J. Lane, A.P. Byrne, and G.D. Dracoulis, Department of Nuclear Physics Annual Report No. ANU-P/1118, 1992 (unpublished).

[6] F. Lidén, A. Johnson, A. Kerek, E. Dafni, and M. Sidi, Nucl. Instrum. Methods Phys. Res. A **273**, 240 (1988).

[7] R.B. Firestone, Nucl. Data Sheets **62**, 101 (1991).

[8] C. Baktash, B. Haas, and W. Nazarewicz, Annu. Rev. Nucl. Part. Sci. **45**, 485 (1995).

[9] F.G. Kondev, G.D. Dracoulis, A.P. Byrne, M. Dasgupta, T. Kibédi, and G.J. Lane, Nucl. Phys. **A601**, 195 (1996).

[10] P. Moller, J.R. Nix, W.D. Myers, and W.J. Swiatecki, At. Data Nucl. Data Tables **59**, 185 (1995).

[11] W. Nazarewicz, M.A. Riley, and J.D. Garrett, Nucl. Phys. **A512**, 61 (1990).

[12] Kirain Jain, O. Burglin, G.D. Dracoulis, B. Fabricius, N. Rowley, and P.M. Walker, Nucl. Phys. **A591**, 61 (1995).

[13] B.D. Jeltema, F.M. Bernthal, T.L. Khoo, and C.L. Dors, Nucl. Phys. **A280**, 21 (1977).